Desalination and Water Treatment
www.deswater.com
15 (2010) 198–204
March
1944-3994 / 1944-3986 © 2010 Desalination Publications. All rights reserved.
doi: 10.5004/dwt.2010.1686

Enhancement of chlorine resistance in carbon nanotube-based nanocomposite reverse osmosis membranes

Junwoo Park, Wansuk Choi, Sung Hyun Kim, Byung Hee Chun, Joona Bang*, Ki Bong Lee*

Department of Chemical & Biological Engineering, Korea University, Anam-dong, Seongbuk-gu, Seoul, 136-713, Korea
Tel. +82 (2) 3290-4851; Fax +82 (2) 926-6102; email: kibonglee@korea.ac.kr, joona@korea.ac.kr

Received 12 November 2009; Accepted in revised form 24 December 2009

ABSTRACT

Aromatic polyamide membranes, which are prepared by interfacial polymerization of m-phenylene diamine (MPDA) in water solution and trimesoyl chloride (TMC) in organic solution, have been widely used as reverse osmosis (RO) membranes for desalination of seawater. However, it has been pointed out that polyamide RO membranes have weak resistance to chlorine, causing deteriorated separation performance. In this study, nanocomposite RO membranes containing multi-walled carbon nanotube (MWCNT) were developed to enhance the chlorine resistance of polyamide membranes. The resulting membranes were analyzed and tested to see the desalination performance. Nonionic surfactant (Triton-X-100) was used in the interfacial polymerization of organic/inorganic nanocomposite RO membranes to improve the dispersion of MWCNTs in the polymer matrix. Scanning electron microscopy (SEM) images and X-ray diffraction (XRD) spectra confirmed that MWCNTs were uniformly distributed in the polymer matrix. When 0.1–1 wt% of MWCNTs were added to polyamide RO membranes, chlorine resistance was measurably improved compared to the conventional polyamide membranes.

Keywords: Desalination; Reverse osmosis membrane; Nanocomposite membrane; Multi-walled carbon nanotube; Chlorine resistance

1. Introduction

Shortage of drinking and usable water has been a significant issue in the world. For solution of the water problem, seawater desalination process using membranes is receiving more and more interest and is being actively developed for commercial use [1–4]. Since 1960s when the study of desalination of seawater began, unsymmetrical cellulose acetate (CA) membranes and polyamide (PA) membranes were used as reverse osmosis membranes to produce pure water from seawater [5].

CA membranes are hydrophilic and have a merit of strong resistance to biofouling. However, they have inferior mechanical strength, weak resistance to chemicals, and narrow operation range for pH. These disadvantages cause decreasing of membrane separation performance in a long-term operation. Currently, PA-based membranes are widely used because they have relatively good endurance and excellent membrane separation performance with more than 99% salt rejection [6–8]. PA membranes,

* Corresponding author.

Presented at SeaHERO Academic Workshop on Development and Optimization of SWRO Desalination Systems
Korea University, Seoul, Korea, November 13–14, 2009

however, show low permeate flux and biofouling problem, especially weak resistance to chlorine due to the structure of amide bond in the main chain [9–11].

To improve the chlorine resistance of PA membranes, various studies were carried out, such as the coating of PA membrane surface with chlorine resistant materials and the introduction of functional groups to the amide structure [12–16]. Additionally, nano-scale functional materials were incorporated when selective layers on the support membrane were interfacially polymerized. For example, dendrimers, nanoparticles, nanoporous polymers, graphene, and carbon nanotube were used as the functional materials to produce thin film nanocomposite (TFN) membranes. The TFN membrane was suggested as a new reverse osmosis polymer membrane that can increase water permeation without sacrificing salt rejection [17–21].

Among nano materials, carbon nanotube (CNT) that was discovered by Iijima Sumio in 1991 shows exceptional mechanical, optical, and electrical properties and has been used in broad areas of chemistry, physics, and engineering fields. Especially, CNT is studied intensively in the areas of nano-probe, display, sensor, drug delivery, filter, electrode of lithium battery, and energy storage [22–30]. In the application of CNT to water treatment membranes, CNTs in a membrane can form numerous small pores to enhance water permeation with keeping high separation ability. Many studies based on numerical simulations and experiments support the great potential of CNT for the water treatment membranes [31–34].

With the expectation of improvement of water treatment membranes using CNT, there is a new issue on the relation of heavy metal and CNT. Recent studies have shown that heavy metals can combine with CNT and then the CNT displays the behavior as potential carriers of toxic pollutants [35,36]. However, the adsorption of heavy metals on CNT does not have only negative aspect. The increase of heavy metal adsorption on CNT implies that it can be used for the removal of heavy metals from water. Therefore, by using these characteristics adequately, CNT can be efficiently applied to water treatment membranes with additional advantages.

In this study, multi-walled carbon nanotubes were used to develop novel high-performance reverse osmosis (RO) membranes for seawater desalination. The deteriorated membrane performance in the conventional PA RO membrane caused by the decomposition of amide bond in the selective layer by chlorine was improved using a CNT/interfacial crosslinking polymerization method. A method to uniformly disperse CNTs through the selective layer of RO membrane was developed. The organic/inorganic nanocomposite RO membranes were experimentally tested and the results showed that the chlorine resistance was measurably enhanced by introducing CNT.

2. Materials and methods

2.1. Materials

m-phenylene diamine (MPDA, >99%, Sigma–Aldrich) was used in the preparation of aqueous solution for interfacial polymerization and multi-walled carbon nanotubes (MWCNTs; ILJIN CNT, average diameter 9–12 nm, average length 10–15 μm) were used as additives. Triethylamine (TEA, 99.5%, Aldrich) was used as the acid acceptor to neutralize HCl produced in the procedure of condensation polymerization. For the solvent of aqueous solution, deionized water (Milli-Q water, 18 MΩ·cm) was used. In the organic solution, trimesoyl chloride (TMC, 98%, Sigma–Aldrich) and n-hexane (95%, Aldrich) were used for monomer and solvent, respectively. Porous polysulfone membranes (Trisep, UE50, MW 100,000 g/mol) were used as supports. For a surfactant, Triton X-100 (non-ionic, Aldrich) was used. All materials were kept in a desiccator before use. The aqueous solution used for RO membrane performance tests was prepared by dissolving sodium chloride (NaCl, 99%, Aldrich) in deionized pure water. For chlorine resistance tests, sodium hypochloride (NaOCl, 4% solution, Aldrich) solution was used.

2.2. Dispersion of multi-walled carbon nanotubes (MWCNTs)

Nano-size materials tend to aggregate due to the van der Waals interaction. To prevent aggregation and uniformly disperse MWCNTs in the polymer matrix, a surfactant, Triton X-100, was added in the deionized water solvent in the procedure of interfacial polymerization. For enhanced dispersion of MWCNTs, the solution was sonicated at a 40 kHz frequency in the ultrasonic cleaner (Branson model B5510-MT) for 6 h at 25°C.

2.3. Preparation of organic/inorganic nanocomposite RO membranes

2.3.1. Support membrane

Polysulfone support membranes were purchased from TriSep Corp. for the preparation of RO membranes. Polysulfone is cheap and stable both mechanically and thermally so it is commonly used as support membrane. The support membranes used were polysulfone ultrafiltration membranes where polysulfone was unsymmetrically coated at 50 μm in depth onto the polyester non-woven surface of 150 μm. The salt rejection in the support membranes was 0%.

2.3.2. Membrane formation

Fig. 1 shows the procedure to make organic/inorganic nanocomposite RO membranes by the interfacial polymerization of MWCNT/MPDA in aqueous solution and TMC in organic solution. First, MWCNT/MPDA aqueous solution is prepared and surfactant is added to

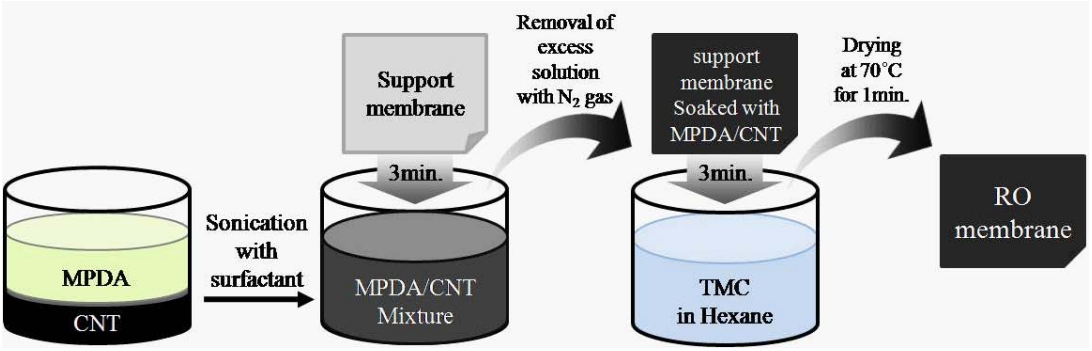

Fig. 1. Schematic diagram of preparation of organic/inorganic nanocomposite RO membrane.

the solution. The solution is sonicated for MWCNT to be uniformly dispersed. Then, the support membrane is soaked in the MWCNT/MPDA mixture solution for 3 min. The support membrane is taken out from the solution and excess solution remained on the membrane surface is removed by blowing with nitrogen gas (if the excess solution is not removed, selective layers would not form stably on the support membrane, resulting in uneven layers after the interfacial polymerization). The support membrane soaked in MWCNT/MPDA solution is quickly immersed in the TMC organic solution to generate selective layers on the membrane surface by interfacial polymerization. The interfacial polymerization occurs within several seconds. After 3 min, the membrane is taken out from the organic solution, washed with deionized water, and dried in the oven at 70°C for 1 min. The prepared organic/inorganic nanocomposite RO membranes are kept in deionized water. The following details show the amount of materials used and the concentration of solutions in the interfacially-polymerized conventional RO membranes and organic/inorganic nanocomposite RO membranes:

- Aqueous solution for interfacially-polymerized conventional RO membrane: 10 g MPDA / 5 g TEA / 485 mL deionized water [2% (w/v) MPDA].
- Aqueous solution for organic/inorganic nanocomposite RO membrane: 5, 25, 50, 250 mg of MWCNT in 10 g MPDA / 5 g TEA / 485 mL deionized water [0.1, 0.5, 1, 5% (w/v) in the aqueous solution of 2% (w/v) MPDA].
- Organic solution for both membranes: 0.5 g TMC / 500 mL n-hexane [0.1% (w/v) TMC in n-hexane].

2.4. Membrane characterization

The surface images of prepared membranes were obtained and characterized using a field emission-scanning electron microscopy (FE-SEM, Hitachi S-4300). The membrane samples were vacuum dried for more than 12 h and coated with platinum (Pt) using a Pt-sputter coater (Hitachi E-1030) before characterization. Organic/inorganic nanocomposite RO membranes and interfacially-polymerized conventional RO membrane were compared, and the generation of selective layers from interfacial polymerization was confirmed from SEM results. SEM images can show surface smoothness/roughness and density of molecules in the selective layers.

X-ray diffraction (XRD) patterns of samples were recorded using a Rigaku x-ray diffractometer (Rigaku D/Max-2500V/PC) with Cu KR radiation operated at 40 kV and 100 mA. The scan range was from 5° to 50° and the XRD patterns were taken at room temperature. XRD analysis can identify crystal structures of MWCNTs in the membrane.

2.5. Test of membrane separation performance

Permeate flux and salt rejection were measured to test membrane separation performance. 2,000 ppm NaCl aqueous solution was used as feed and the test experiments were performed at pH 7, 225 psig (15.5 bar) feed pressure, and 25±2°C (77°F) temperature. A circle membrane with 5.2 cm diameter was set in the test cell and the feed solution flowed through the membrane. Fig. 2 shows the picture of a homemade test cell to measure permeate flux and salt rejection in RO membranes. To optimize the test conditions, tests were started after a 30 min stabilization stage for the compensation of the operating pressure. After the test conditions were stabilized, the permeate solution was sampled every 10 min and its electrical conductance was measured by a conductivity meter (PC650, EUTECH). The amount and conductance of the permeate were used to calculate the permeate flux using Eq. (1) and salt rejection using Eq. (2).

$$\text{Flux} = \frac{\text{permeate (L)}}{\text{membrane area (m}^2\text{)} \times \text{time (h)}} \quad (1)$$

$$\text{Rejection (\%)} = \left(1 - \frac{\text{permeate conductance}}{\text{feed conductance}}\right) \times 100 \quad (2)$$

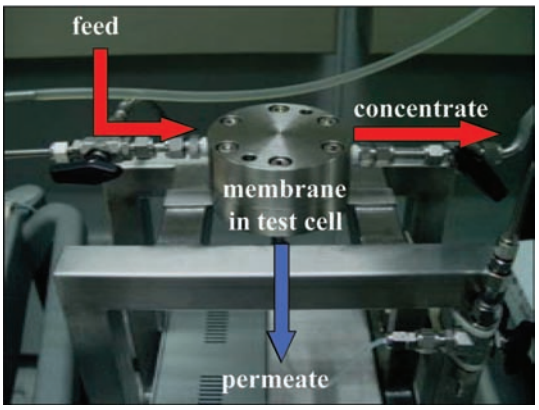

Fig. 2. Picture of the test cell for membrane separation performance.

3. Results and discussion

3.1. Membrane characterization

Fig. 3 shows SEM images of the surface of the interfacially-polymerized conventional RO membrane and organic/inorganic nanocomposite RO membranes. The SEM images provide the information on the surface morphology of the membrane and the existence of MWCNT particles in the surface layers. The surface of the conventional PA RO membrane appears to be uniform, exhibiting hill and valley microstructure morphology (Fig. 3a). In Figs. 3b–d, it can be seen that an incorporation of MWCNT significantly changed the surface morphology of the membranes compared to that of the conventional PA membrane. Interestingly, it can be clearly observed that the period of hill and valley increases as the amount of MWCNT loading increases. This is probably due to the incorporation of long MWCNT strands in the membranes during interfacial polymerization. The uniform morphology in the organic/inorganic nanocomposite RO membranes implies uniform distribution of MWCNT in the selective layers.

Fig. 4 compares XRD patterns of pristine MWCNT and organic/inorganic nanocomposite RO membrane. The scan range of x-ray in diffractometry was from 5° to 50° but no distinguishable peak was found at a low angle. The XRD pattern of pristine MWCNT shows two characteristic peaks at 38.3° and 44.6°. Theses two peaks can be seen also in the XRD pattern of organic/inorganic nanocomposite RO membrane, implying that MWCNT remained well in the membrane prepared.

3.2. Effect of MWCNT loadings on membrane separation performance

Several organic/inorganic nanocomposite RO membranes with different MWCNT loadings were tested to examine the effect of MWCNT loadings on the RO membrane performance and to find the optimal composition of the RO membrane. The tested MWCNT loadings were 0.1, 0.5, 1, and 5% (w/v). As the amount of MWCNT loadings

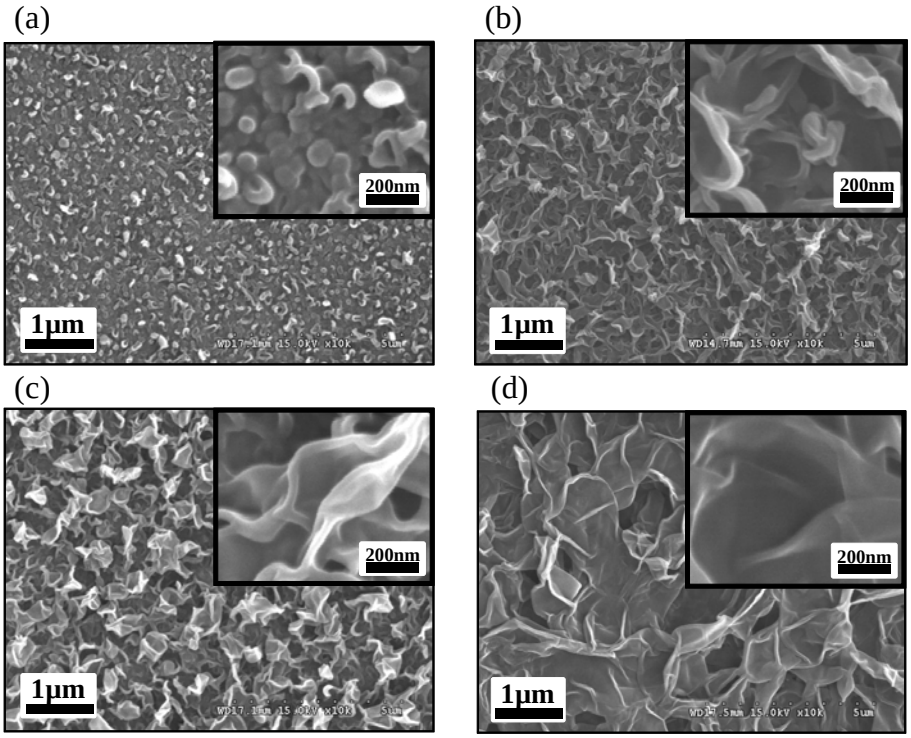

Fig. 3. SEM images of surface of (a) interfacially-polymerized conventional RO membrane; organic/inorganic nanocomposite RO membranes with MWCNT loading of (b) 0.1%, (c) 0.5%, and (d) 1% (w/v).

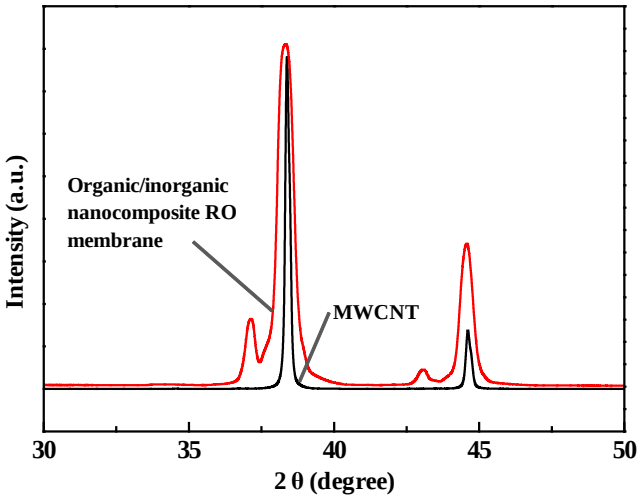

Fig. 4. XRD patterns of pristine MWCNT and organic/inorganic nanocomposite RO membrane.

increased, it was clearly observed with the naked eye that the membranes became darker. MWCNTs are graphitic materials whose colors are black. Therefore, the darker color of the membrane indicates that the membrane contains more MWCNTs.

Fig. 5 shows the permeate flux and salt rejection with time for the interfacially-polymerized conventional RO membrane and organic/inorganic nanocomposite RO membranes. For all experiments, the ionic salt (NaCl) concentration and flux in the feed water were fixed to 2,000 ppm and 333 L/m^2·h, respectively. After operating for ~30 min, all RO membranes maintained stable separation performance. It was observed that both permeate flux and salt rejection were slightly decreased when MWCNT was added but salt rejection was more than 92% for 0.1, 0.5, 1% (w/v) of MWCNT loadings meaning that the membrane separation performance was within a reasonably acceptable range. For the organic/inorganic nanocomposite RO membranes, as MWCNT loadings increased, the permeate flux increased [from 11.1 L/m^2·h at 0.1% (w/v) of MWCNT to 13.6 L/m^2·h at 1% (w/v) of MWCNT] but salt rejection decreased [from 93.4% at 0.1% (w/v) of MWCNT to 92.5% at 1% (w/v) of MWCNT]. This is presumably caused by an increasing number of pores in the RO membranes with MWCNT loadings. More pores can allow the solution to permeate easily but at the same time the salt permeation also increases. When MWCNT loading was 5% (w/v), the permeate flux and salt rejection were 35 L/m^2·h and 46%, respectively. In this case, too much MWCNT in the MPDA solution prevents the formation of densely-crosslinked amide network during interfacial polymerization. Consequently, relatively large pores between MWCNTs are produced resulting in high permeate flux but poor separation. From these results, it can be concluded that the reasonable MWCNT loadings in MPDA solution for the interfacial polymerization with TMC organic solution are in the range of 0.1–1% (w/v).

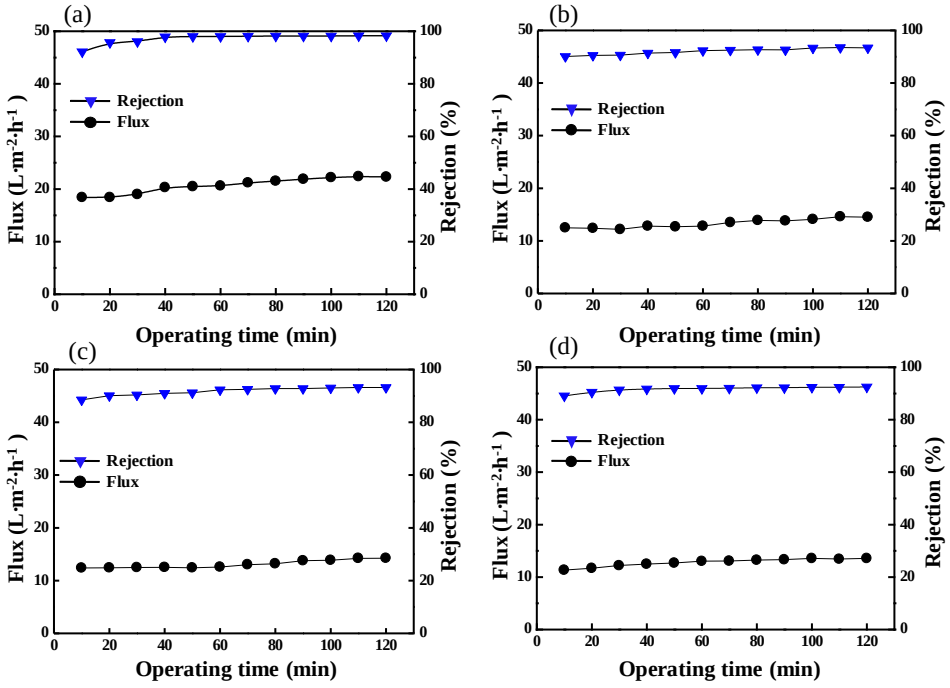

Fig. 5. Permeate flux and salt rejection of (a) interfacially-polymerized conventional RO membrane; organic/inorganic nanocomposite RO membranes with MWCNT loading of (b) 0.1%, (c) 0.5%, and (d) 1% (w/v).

3.3. Chlorine resistance

3,000 ppm NaOCl solution was used to investigate the effect of MWCNT on the RO membrane stability against chlorine. Both interfacially-polymerized conventional RO membrane and organic/inorganic nanocomposite RO membranes were prepared following the aforementioned methods. The prepared membranes were initially tested with 2,000 ppm NaCl feed solution in the test condition for membrane separation performance aforementioned. Then, the tested membranes were soaked in 3,000 ppm NaOCl solution for 4 h. After washing with deionized water, the membranes were tested again with 2,000 ppm NaCl feed solution to see the change in membrane separation performance.

Fig. 6 represents the stability against chlorine for RO membranes immersed in 3,000 ppm NaOCl solution. The stability can be determined from the change of salt rejection. As can be seen in Fig. 6, for the conventional PA RO membrane, salt rejection decreased from 98.3% to 76.5% after the membrane was soaked in the NaOCl solution. When the PA membrane contacts with chlorine, N–H in the amide bond (–NHCO–) is chlorinated and then hydrolyzed in water. Finally, the amine is changed into a quinoid structure and decomposed. In another mechanism, after chlorination, ions are successively rearranged between aromatic rings connecting with the N–H group and then the above decomposition reactions occur. The deformation of the amide bond in the main chain causes the decomposition of PA selective layers resulting in the degradation of physical properties of the membrane and deteriorated membrane separation performance [9–11].

Fig. 6 also compares the stability against chlorine (or chlorine resistance) between the conventional PA RO membrane and organic/inorganic nanocomposite RO membranes. Before immersing in NaOCl solution, the salt rejection in the conventional PA RO membrane was higher than that in the organic/inorganic nanocomposite RO membranes. However, after exposure to chlorine, the salt rejection in the conventional PA RO membrane decreased more significantly compared to that in the organic/inorganic nanocomposite RO membranes. For the PA membrane, the salt rejection decreased by 21.8% (from 98.3% to 76.5%) after chlorination. However, nanocomposite membranes exhibited a decrease in the salt rejection by 15.8% (from 93.4% to 77.6%), 11.2% (from 93.2% to 82.0%), and 10.1% (from 92.5% to 82.4%), for 0.1, 0.5, 1% (w/v) of MWCNT loadings, respectively. Therefore, as the amount of MWCNT loading increased, the stability against chlorine appeared to be improved. It is thought that the interaction between the carboxylic group of the modified MWCNTs in polymer matrix and the amide bond generated in the interfacial polymerization makes the membranes more stable against chlorine. The results of salt rejection change clearly show that organic/inorganic nanocomposite RO membranes are more stable against chlorine than the conventional PA RO membrane.

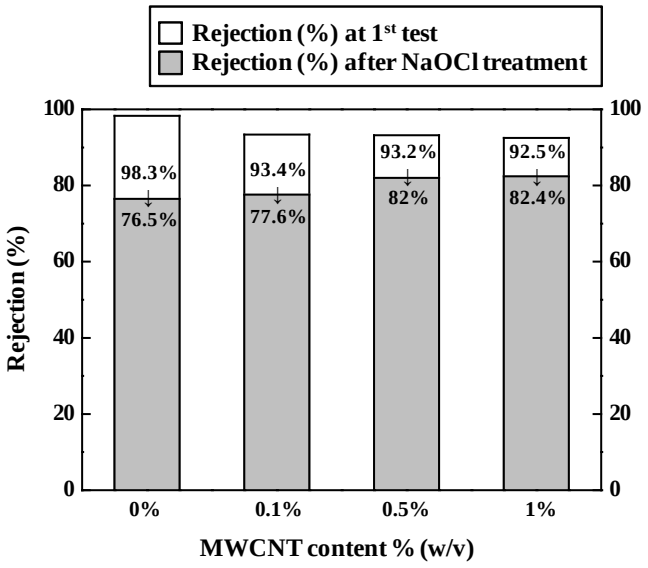

Fig. 6. Change of salt rejection after immersing in 3,000 ppm NaOCl aqueous solution.

4. Conclusions

In this study, organic/inorganic nanocomposite RO membranes were prepared by the interfacial polymerization of MWCNT-dispersed MPDA aqueous solution and TMC organic solution. SEM images and XRD spectra showed that MWCNT existed uniformly in the polymer matrix. Initially, the permeate flux and salt rejection in the conventional PA RO membrane were higher than those in the organic/inorganic nanocomposite RO membranes. However, after the exposure to high concentration NaOCl solution, salt rejection in the organic/inorganic nanocomposite RO membranes appeared to surpass that of the conventional PA RO membrane. This implies that MWCNT loading to the PA membrane can enhance the stability against chlorine (or chlorine resistance). In the MWCNT loading range of 0.1–1% (w/v), chlorine resistance of organic/inorganic nanocomposite RO membranes was improved as the amount of MWCNT increased.

CNT has been studied to improve physical properties and even to generate new characteristics of materials. This study showed that application of CNT can be a solution to the limitation of the polyamide RO membrane due to its weak chlorine resistance. Moreover, the simple preparation procedure of organic/inorganic nanocomposite RO membranes will facilitate the bulk production of RO membranes.

Acknowledgements

This research was supported by a grant (07seaheroB02-03) from the Plant Technology Advancement

Program funded by the Ministry of Land, Transport and Maritime Affairs of the Korean government.

References

[1] C.Y. Tang, Y.-N. Kwon and J.O. Leckie, Effect of membrane chemistry and coating layer on physiochemical properties of thin film composite polyamide RO and NF membranes: I. FTIR and XPS characterization of polyamide and coating layer chemistry, Desalination, 242 (2009) 149–167.

[2] R.J. Petersen, Composite reverse osmosis and nanofiltration membranes, J. Membr. Sci., 83 (1993) 81–150.

[3] C.R. Bartels, M. Wilf, K. Andes and J. Iong, Design considerations for wastewater treatment by reverse osmosis, Water. Sci. Technol., 51 (2005) 473–482.

[4] K. Leung, Ion-dipole interactions are asymptotically unscreened by water in dipolar nanopores, yielding patterned ion distributions, J. Am. Chem. Soc., 130 (2008) 1808–1809.

[5] S. Loeb and S. Sourirajan, UCLA Department of Engineering Report 60-60, 1962.

[6] R.W. Baker, Membrane Technology and Application, Wiley, New York, 2004.

[7] H.K. Lonsdale, Recent advances in reverse osmosis membranes, Desalination, 13 (1973) 317–332.

[8] J. Araki and S. Kuga, Effect of trace electrolyte on liquid crystal type of cellulose microcrystals, Langmuir, 17 (2001) 4493–4496.

[9] R. Singh, Polyamide polymer solution behavior under chlorination conditions, J. Membr. Sci., 88 (1994) 285–287.

[10] M. Kurihara, T. Uemura, Y. Himeshima, K. Ueno and R. Bairinji, Development of crosslinked aromatic polyamide composite reverse osmosis membrane, J. Chem. Soc. Jpn., 2 (1994) 97–107.

[11] A.E. Bradfield, L.H.N. Cooper and K.J.P. Orton, CCCLXXXII — The halogenation of p-hydroxydiphenylamine. Part II, J. Chem. Soc., (1927) 2854–2864.

[12] L.D. Kershner, C.E. Reineke, N. Sarkar and L.R. Wilson, Water-insoluble, crosslinked, sulfonated aromatic polyamide, US Patent 4,824,916, 1986.

[13] P.R. Buch, D.J. Mohan and A.V.R. Reddy, Preparation, characterization and chlorine stability of aromatic–cycloaliphatic polyamide thin film composite membranes, J. Membr. Sci., 309 (2008) 36–44.

[14] S. Konagaya, K. Nita, Y. Matsui and M. Miyagi, New chlorine-resistant polyamide reverse osmosis membrane with hollow fiber configuration, J. Appl. Polym. Sci., 79 (2001) 517–527.

[15] S. Konagaya, H. Kuzumoto and O. Watanabe, New reverse osmosis membrane materials with higher resistance to chlorine, J. Appl. Polym. Sci., 75 (2000) 1357–1364.

[16] J. Glater, S.-K. Hong and M. Elimelech, The search for a chlorine-resistant reverse osmosis membrane, Desalination, 95 (1994) 325–343.

[17] B.-H. Jeong, E.M.V. Hoek, Y. Yan, A. Subramani, X. Huang, G. Hurwitz, A.K. Ghosh and A. Jawor, Interfacial polymerization of thin film nanocomposites: A new concept for reverse osmosis membranes, J. Membr. Sci., 294 (2007) 1–7.

[18] L. Lianchao, W. Baoguo, T. Huimin, C. Tianlu and X. Jiping, A novel nanofiltration membrane prepared with PAMAM and TMC by in situ interfacial polymerization on PEK-C ultrafiltration membrane, J. Membr. Sci., 269 (2006) 84–93.

[19] M. Zhou, P.R. Nemade, X. Lu, X. Zheng, E.S. Hatakeyama, R.D. Noble and D.L. Gin, New type of membrane material for water desalination based on a cross-linked bicontinuous cubic lyotropic liquid crystal assembly, J. Am. Chem. Soc., 129 (2007) 9574–9575.

[20] K. Sint, B. Wangand P. Král, Selective ion passage through functionalized graphene nanopores, J. Am. Chem. Soc., 130 (2008) 16448–16449.

[21] B. Corry, Designing carbon nanotube membranes for efficient water desalination, J. Phys. Chem. B, 112 (2008) 1427–1434.

[22] R.H. Baughman, A.A. Zakhidov and W.A. De Heer, Carbon nanotubes — the route toward applications, Science, 297 (2002) 787–792.

[23] B.I. Yakobson and R.E. Smalley, Fullerene nanotubes: C1,000,000 and beyond, Am. Sci., 85 (1997) 324–337.

[24] P.M. Ajayan, Nanotubes from carbon, Chem. Rev., 99 (1999) 1787–1800.

[25] A. Javey, Ballistic carbon nanotube field-effect transistors, Nature, 424 (2003) 654–657.

[26] M.S. Arnold, A.A. Green, J.F. Hulvat, S.I. Stupp and M.C. Hersam, Sorting carbon nanotubes by electronic structure using density differentiation, Nature Nanotechnol., 1 (2006) 60–65.

[27] A.R. Naeemi, R. Sarvari and J.D. Meindl, Performance comparison between carbon nanotube and copper interconnects for gigascale integration (GSI), IEEE Electron. Device Lett., 26 (2005) 84–86.

[28] H.F. Mark, N. Bikales, C.G. Overberger, G. Menges and J.I. Kroschwitz, Encyclopedia of Polymer Science and Engineering, 2nd ed, vol. 8, Wiley, New York, 1985.

[29] P. Couvreur, G. Barratt, E. Fattal, P. Legrande and C. Vauthier, Nanocapsule technology: a review, Crit. Rev. Therap. Drug Carrier Systems, 19 (2002) 99–134.

[30] S.-S. Fan, K.-L Jiang, L. Liu, C. Feng and X.-B. Zhang, Carbon nanotube film structure and method for fabricating the same, US20080248235, 2008.

[31] G. Cicero, J.C. Grossman, E. Schwegler, F. Gygi and G. Galli, Water confined in nanotubes and between graphene sheets: A first principle study, J. Am. Chem. Soc., 130 (2008) 1871–1878.

[32] A.A. Gusev and O. Guseva, Rapid mass transport in mixed matrix nanotube/polymer membranes, Adv. Mater., 19 (2007) 2672–2676.

[33] S. Joseph and N.R. Aluru, Why are carbon nanotubes fast transporters of water? Nano Lett., 8 (2008) 452–458.

[34] M.J. Longhurst and N. Quirke, Temperature-driven pumping of fluid through single-walled carbon nanotubes, Nano Lett., 7 (2007) 3324–3328.

[35] A. Schierz and H. Zänker, Aqueous suspensions of carbon nanotubes: surface oxidation, colloidal stability and uranium sorption, Environ. Pollut., 157 (2009) 1088–1094.

[36] L. McJilton, C. Horton, C. Kittrell, D. Ogrin, H. Peng, F. Liang, W.E. Billups, H.K. Schmidt, R.H. Hauge, R.E. Smalley and A.R. Barron, Nebulization of single-walled carbon nanotubes for respiratory toxicity studies, Carbon, 47 (2009) 2528–2530.